ELSEVIER

Journal of Chromatography A, 859 (1999) 121–132

JOURNAL OF CHROMATOGRAPHY A

www.elsevier.com/locate/chroma

Shape-selective separation of polycyclic aromatic hydrocarbons on protoporphyrin-silica phases
Effect of surface porphyrin distribution on column efficiency

Shaohua Chen, Ulrich Ruedel, Mark E. Meyerhoff*

Department of Chemistry, The University of Michigan, Ann Arbor, MI 48109-1055, USA

Received 4 May 1999; received in revised form 30 July 1999; accepted 30 July 1999

Abstract

The chromatographic performance of various metalloprotoporphyrin-silica (MProP-silica) packing materials prepared using different porphyrin immobilization schemes is examined. Column efficiency and solute resolution for the shape-selective separation of polycyclic aromatic hydrocarbons (PAHs) can be improved significantly by preparing phases with lower porphyrin coverages and with a more homogeneous distribution of the porphyrin species on the surface. The latter is accomplished by spreading/diluting the number of aminopropyl reactive sites on the silica surface via mixing an inert methyltrimethoxysilane with 3-aminopropyltriethoxysilane during this preliminary reaction step. Subsequent covalent attachment of the ProP via amide bonds to the pendant amine sites results in a more even distribution of the porphyrins on the surface. Band shapes and retention times as a function of injected solute concentration as well as HPLC separation of various test mixtures of PAHs (including standard reference material SRM 869) are used to confirm the enhanced performance of these so-called ''spread'' phases. Changes in the nature of the immobilized porphyrin distribution on the silica surface are further probed by a coupled redox/UV–Vis absorbance method, and results suggest a decrease in the number of ProP species immobilized as aggregates on the surface.

Keywords: Stationary phases, LC; Protoporphyrin-silica stationary phases; Metalloprotoporphyrin-silica stationary phases; Porphyrin-silica stationary phases; Polycyclic aromatic hydrocarbons

1. Introduction

Chemical modification of silica packing materials remains a popular approach to achieve novel solute selectivity in high-performance liquid chromatography [1–5]. Protoporphyrin (ProP)-silica and metalloprotoporphyrin (MProP)-silica are new HPLC stationary phases prepared recently in our laboratory [6]. These materials already have exhibited extraordinary shape selectivity in the separation of polycyclic aromatic hydrocarbons (PAHs) and other related π-rich solutes [7]. Since the macrocycle of protoporphyrin is planar, ProP-silicas offer unprecedented retention selectivity for planar PAHs over non-planar PAHs. Interestingly, it has been found that the nature of the central metal ion of the immobilized porphyrin structure also plays a significant role in the retention and solute shape selectivity achieved on MProP-silica phases. This property can also be employed to tune the solute selectivity exhibited when such phases are employed as immobilized metal ion affinity supports for the sepa-

*Corresponding author. Fax: +1-734-763-5916.

0021-9673/99/$ – see front matter
PII: S0021-9673(99)00840-7

ration of amino acids and peptides [8]. Indeed, it has been demonstrated that peptides rich in L-tryptophan and L-histidine residues are retained to a much higher degree on Cu(II)ProP-silica compared to structures with other metal ion centers.

Unfortunately, while MProP-silica materials offer very unique and useful solute selectivities, columns packed with such phases often exhibit unsatisfactory efficiencies ($N<1000/m$) and significant peak tailing (i.e., high asymmetry factors for solute bands), especially for highly retained solutes. It is an important task, therefore, to understand the interaction mechanisms responsible for such behavior so that the inherent selectivity of these phases can be fully realized in chromatographic separations and analysis. Over the years, many studies have demonstrated that changing the immobilization procedure or changing the distribution of stationary phase ligands on silica supports can result in significant improvements in chromatographic behavior [5,9–11]. For example, C_{18}-silica phases are the best characterized materials and many investigators have found that ligand loading, ligand distribution, and the orientation and entanglement of the alkyl chains on the surface all play important roles in the selectivity and efficiency exhibited by these stationary phases (e.g., polymeric C_{18} vs. monomeric C_{18} [10]). Therefore, it is reasonable to assume that similar studies of the MProP-silica phases could also lead to a better understanding of the factors that have limited their chromatographic performance thus far.

It is known that band broadening and peak tailing in HPLC can occur when a solute species can interact with a number of different sites on the stationary phase, each with a different solute–stationary phase equilibrium binding constant and/or different kinetic constants for ''on'' and ''off'' rates [12,13]. Hence, is it reasonable to assume that a heterogeneous distribution of porphyrins on the silica surface could play a role in the band broadening observed on MProP-silica phases. In fact, ProP is a planar π-rich molecule that is well known to aggregate in solution via intermolecular $\pi-\pi$ interaction/stacking [14]. It is possible, therefore, that after chemical immobilization of ProP, the silica surface is covered with a distribution of porphyrin aggregate clusters (of different size) rather than a homogeneous distribution of monomeric porphyrin structures (see Fig. 1A). Such a surface structure would likely contribute to the inefficiencies observed.

Herein we attempt to assess the role of MProP distribution on the surface of the silica by utilizing alternate immobilization schemes to help prevent covalent attachment of intact aggregate structures. Two approaches are examined: (1) diluting the concentration of porphyrin used during the immobilization reaction; and (2) diluting the initial surface distribution of amine sites on the silica packing so

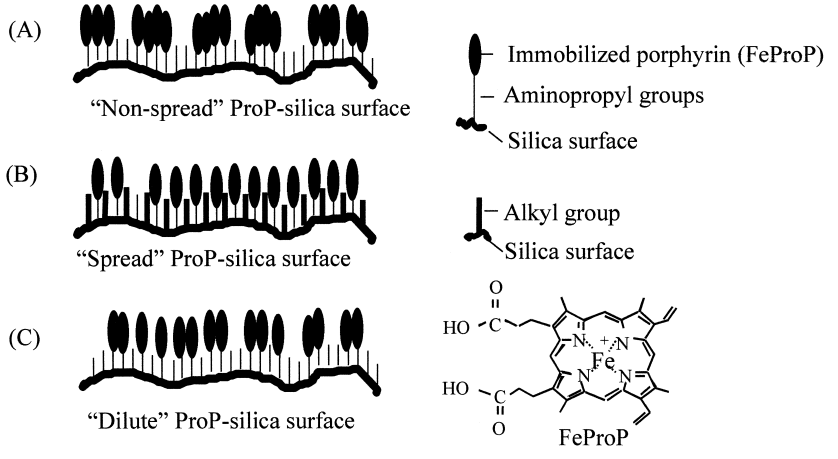

Fig. 1. Schematic diagram of possible porphyrin distribution on ProP-silica phases representing different porphyrin immobilization schemes. (A) The ''normal'' FeProP-silica phases; (B) the ''spread'' FeProP-silica phases; (C) the ''dilute'' silica phases.

that subsequent covalent linkage of the porphyrin ligand will not result in adjacent immobilized ProP species that retain their aggregate structures. It will be shown that the latter synthetic approach results in phases that exhibit significant improvements in peak efficiency and tailing factors while maintaining a high degree of planar vs. non-planar shape selectivity. It will also be shown that a simple coupled redox/UV–Vis absorbance method can be used to qualitatively characterize the distribution of ProP species on the silica surface.

2. Experimental

2.1. Reagents

Protoporphyrin IX (ProP) was purchased from Midcentury Chemicals (Posen, IL, USA). Hyperprep 8 μm silica gel with a surface area of 90 m^2/g and a pore size of 300 Å was a product of Keystone Scientific (Bellefonte, PA, USA). Aminopropyltriethoxylsilane was obtained from Hüls (Piscataway, NJ, USA). Other silanization reagents (methyltrimethoxysilane, ethyltrimethoxysilane), hemin [chloroprotoporphyrin IX iron(III)], sodium dodecyl sulfate (SDS), anhydrous dimethylformamide (DMF) used in the immobilization of ProP, and HPLC-grade DMF employed in the metallation of protoporphyrin-silica, were purchased from Aldrich (Milwaukee, WI, USA). HPLC-grade acetonitrile was from Mallinckrodt (Paris, KY, USA). The coupling reagent, 1,1′-carbonyldiimidazole (CDI), was a product of Fluka (Ronkonkoma, NY). HPLC grade methanol and acetonitrile utilized as mobile phases were purchased from Aldrich. Doubly deionized water was filtered through a 0.45 μm polypropylene membrane from Alltech Associates (Deerfield, IL, USA) prior to use in preparing various mobile phases.

Standard reference material (SRM 869) was a generous gift from Dr. L. Sander at The National Institute of Standards and Technology. Naphthalene, biphenyl, *o*-terphenyl, phenanthrene, anthrancene, triphenylene, pyrene, chrysene, perylene, benzo[*a*]pyrene were obtained from Aldrich. 1,1-Binaphthyl was purchased from Acros Organics (Fisher Scientific, Pittsburgh, PA, USA).

2.2. Preparation of the protoporphyrin- and metalloprotoporphyrin-silica stationary phases

A detailed procedure for synthesizing the traditional ProP-silica and MProP-silica stationary phases was described previously [6]. In this work, three different immobilization methods were employed (see below). In each case, the coverage of amino groups on the silica surface after the initial silanization with 3-aminopropyltriethoxysilane was determined by the relative increase in nitrogen content as measured by elemental analysis of the material before and after the reaction [15]. The final coverage of ProP was determined in a similar manner. All excess amino groups were end-capped by refluxing the silica gel with acetic anhydride for 1 h before being packed into HPLC columns.

2.2.1. Synthesis of ''normal'' FeProP-silica phases

The ''normal'' phases (see Fig. 1A for pictorial representation of resulting phase) were prepared as described in earlier work [6]. Briefly, the silica gel was first reacted with excess 3-aminopropyltriethoxysilane (ten-fold in excess of the necessary amount assuming a maximum surface coverage of 8 $\mu mol/m^2$) in toluene to obtain the aminopropyl-silica. ProP (five-fold in excess of the amine coverage on silica surface after the 3-aminopropyltriethoxysilane treatment) was then activated with CDI (2 equivalents per ProP) in DMF, and reacted with the aminopropyl-silica to form ProP-silica via amide bonds between the porphyrin and the surface amine groups. The excess amine groups were then end-capped by refluxing the silica gel with acetic anhydride. Each of the phases was then metallated with Fe(III) by refluxing with $FeCl_3 \cdot 6H_2O$ (10 times in excess of the immobilized porphyrin) in 50 ml DMF for 4 h.

2.2.2. Synthesis of ''spread'' FeProP-silica phases

''Spread'' phases were synthesized by refluxing the silica gel (2 g) with a mixture of 3-aminopropyltriethoxysilane and methyltrimethoxysilane (approximately 1:3 molar ratio to achieve the optimal result in ''spreading'') in 25 ml toluene for 6 h. Thus, the amine groups were spread out over the silica surface and immobilization of clustered porphyrin aggregates during the subsequent immobiliza-

tion step was less likely (see Fig. 1B). The actual amine coverage resulting from the silanization reaction can be controlled by varying the proportion of 3-aminopropyltriethoxysilane and the inert silane used. ProP (0.36 g) was then activated with CDI (0.18 g) first, then reacted with the aminopropyl-silica. End-capping of the unreacted amino groups was performed by refluxing the silica gel in acetic anhydride [15]. Each of the phases was metallated with Fe(III) by refluxing with $FeCl_3 \cdot 6H_2O$ (10 times in excess of the immobilized porphyrin) in 50 ml DMF for 4 h.

2.2.3. Synthesis of ''dilute'' FeProP-silica phases

Aminopropyl-silica was prepared as above for the ''normal'' ProP-silica. However, the subsequent immobilization of ProP was performed using an extremely dilute solution of porphyrin in DMF (~4×10^{-3} *M*). In this manner, the number and size of porphyrin aggregates bound covalently to the surface of the silica was hopefully diminished (see Fig. 1C). Porphyrin immobilization was performed in a similar manner as for the ''normal'' phases.

2.3. Column packing

ProP-silica gel was sifted through a 15 μm stainless steel screen and packed into a 100 mm×4.6 mm I.D. stainless steel column by the down fill slurry packing method, using toluene–isopropanol (80:20) as slurry solvent and 100% isopropanol as the flow solvent under a packing pressure of 6000 p.s.i. (1 p.s.i.=6894.76 Pa). A 15 μm stainless steel screen was used for the sifting because, although the silica gel has a mean diameter of 8 μm, the particle sizes actually ranged from 6.5 μm to 12.5 μm (based on scanning electron microscope images). A 15 μm sift was therefore the most suitable size screen on-hand to obtain a high yield of the original packing material in a reasonable time period. A total of 200 ml of solvent was eluted from the column during the packing process.

2.4. Instrumentation

The HPLC system consisted of a Spectra-Physics (San Jose, CA, USA) SP 8700 solvent delivery system, a Spectra-Physics SP 4290 computing integrator, a Kratos (Ramsey, NJ, USA) Spectroflow 773 variable-wavelength UV–Vis detector, and a Rheodyne (Cotati, CA, USA) model 7010 sample injection valve with a 20 μl loop. The detector for isotherm experiments was an LC 305 scanning fluorescent detector from Thermo Separation Products (San Jose, CA, USA). A Beckman DU 640B spectrophotometer (Fullerton, CA, USA) was employed to record the UV–Vis spectra of the various ProP-silica phases.

2.5. Characterization of Fe(III)ProP-silica by coupled redox/UV–Vis absorbance method

The UV–Vis spectra of various Fe(III)ProP-silica (1 mg) suspensions in 3 ml of 0.1 *M* sodium hydroxide (with 2.5%, w/w, SDS) were taken from 300 nm to 800 nm. Adding sodium hydrosulfite powder (1 mg) to the suspension reduces the Fe(III)ProP-silica to Fe(II)ProP-silica [16]. A 100 μl volume of pyridine was then added to form the pyridine–ferroporphyrin complex which exhibits much more distinguished Q bands [17]. Spectra of the corresponding Fe(III)ProP-silicas taken prior to reduction and addition of the pyridine were also recorded.

3. Results and discussion

3.1. Effect of synthesis route on column efficiency

To prove that porphyrin aggregation during the immobilization of ProP was at least partially responsible for the inefficiency of previously reported columns packed with MProP-silicas, a series of phases made by each of the methods outlined in the Experimental section were prepared (see Table 1). To better aid in the comparison of these materials, only phases with similar ProP surface coverage after the entire immobilization process were tested in preliminary PAH separations (approx. 0.2 $\mu mol/m^2$: ''spread-4'' 0.20 $\mu mol/m^2$, ''normal-1'' 0.26 $\mu mol/m^2$, and ''dilute-1'' 0.20 $\mu mol/m^2$). Since for PAH solutes, the performance of Fe(III)ProP-silica is representative, in terms of selectivity and efficiency, to other metallated structures, all results reported here were obtained on the Fe(III)ProP-silica materi-

Table 1
Selectivity factors ($\alpha_{Anth/Phe}$) and efficiencies of phenanthrene and anthracene on different FeProP-silica columns using acetonitrile–water (50:50) as mobile phase

FeProP-silica column	Amine coverage ($\mu mol/m^2$)	Porphyrin coverage ($\mu mol/m^2$)	Selectivity factor (α)	Peak efficiency (plates/m)[a]	Peak efficiency (plates/m)[a] (anthracene)
Normal-2	3.62	0.62	1.00	–	–
Normal-3	3.62	1.18	1.27	556	166
Normal-4[b]	4.28	2.27	1.28	302	202
Spread-2	1.97	0.79	1.42	1290	604
Spread-1	1.38	0.85	1.48	2280	1490
Normal-1	4.35	0.26	1.00	–	–
Dilute-1	4.06	0.20	1.23	2680	1800
Spread-3	1.61	0.20	1.26	3570	2310
Spread-4	0.97	0.20	1.23	8570	3570

[a] Plate number was calculated by: $N=5.54(t_r/W_{1/2})^2$; N stands for the peak efficiency; t_r is the retention time; $W_{1/2}$ stands for the half-width of the peak.
[b] Mobile phase changed to acetonitrile–water (80:20) because of the retention was too long using the weaker mobile phase.

als. Table 1 summarizes the specific initial amine content and final porphyrin coverages of most ''normal'', ''spread'' and ''dilute'' phases examined in this work.

A preliminary comparison of the three phases was carried out by separating a test mixture of 12 PAHs using gradient elution. Fig. 2 provides the typical chromatograms obtained for this separation under identical conditions (using packings with similar surface coverage—see above). It is clear that the ''spread-4'' phase offers the greatest resolving power. Indeed, several compounds that were not resolved on the ''normal-1'' Fe(III)ProP-silica phase were baseline resolved (phenanthrene and anthracene, chrysene and triphenylene), or partially resolved (perylene and benzo[*a*]pyrene) on the ''spread-4'' FeProP-silica material. As also shown in Fig. 2, the performance of the ''dilute-1'' Fe(III)-silica phase appears to be somewhere in between that of the ''spread-4'' and ''normal-1'' phases in terms of resolution and band symmetry.

Based on the chromatograms shown in Fig. 2, it is

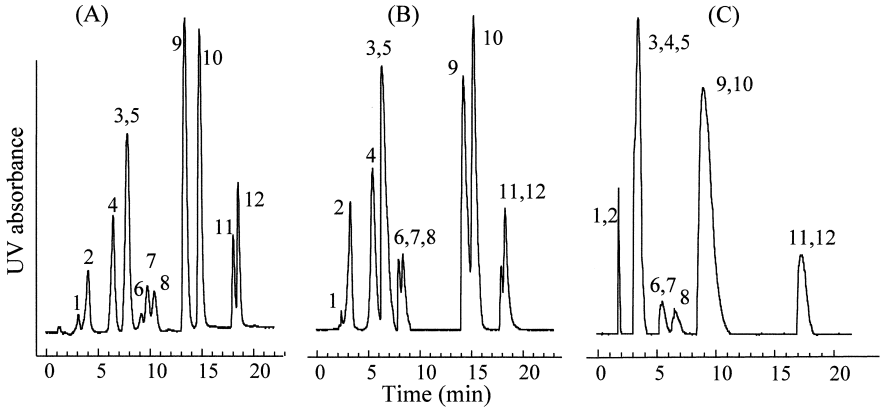

Fig. 2. Separation of 12 PAHs on FeProP-silica: (A) ''spread-4'' phases with coverage (cov) of 0.20 $\mu mol/m^2$; (B) ''dilute-1'' phase (cov=0.20 $\mu mol/m^2$); (C) ''normal-1'' phase (cov=0.26 $\mu mol/m^2$). Solutes are: (1) naphthalene, (2) biphenyl, (3) 1,1-binaphthyl, (4) phenanthrene, (5) anthracene, (6) fluoranthene, (7) pyrene, (8) benz[*a*]anthracene, (9) triphenylene, (10) chrysene, (11) perylene, (12) benzo[*a*]pyrene. Mobile phase: acetonitrile–water (50:50) for 10 min, step to 100% acetonitrile in 10 min. UV detection at 254 nm, flow-rate: 1 ml/min.

also likely that higher efficiency was also obtained on the columns packed with the ''spread-4'' phase since the peak for phenanthrene (peak 4), a reasonably well resolved solute that elutes at about 5 min on both the ''spread-4'' and ''dilute-1'' phases, has a half-width that is smaller on the ''spread-4'' phase than that on ''dilute-1'' material, indicating higher efficiency on ''spread'' phases. Since both the ''normal-1'' and ''spread-4'' Fe(III)ProP-silica phases have similar surface coverage (see Table 1), the reason for the observed difference in column performance may well be related to the differences in the porphyrin immobilization procedure. Another important observation relates to the separation of benz[*a*]anthracene/chrysene pair on ProP-silica phases. This solute pair is normally difficult to separate on monomeric C_{18} phases [20]. A good separation of this solute pair on ProP-silica indicates not only good planarity selectivity for ProP-silica but also high topology selectivity.

Further examination of the different phases with respect to selectivity and efficiency was carried out using phenanthrene and anthracene as test solutes. Similar solute pairs have been used previously to assess the resolution obtainable on other columns employed for PAH separations [18]. To further study the effect of porphyrin surface distribution, different phases with variable loading of amine groups and ProP were prepared using the ''spread'' and ''normal'' synthetic procedures. The selectivity factor for these two solutes on the different materials are compared in Table 1. For Fe(III)ProP-silica phases prepared using the ''normal'' synthesis procedure, the amine coverage on silica surface after the reaction with 3-aminopropyltriethoxysilane is approximately 3.5~4.5 $\mu mol/m^2$. For ''spread'' phases, the amine coverage after the silanization reaction is approximately 0.97~1.97 $\mu mol/m^2$, depending on the proportion of alkylsilane and 3-aminopropylsilane in the reaction. Varying the concentration of porphyrin used in the immobilization step can alter the porphyrin coverage on these phases. It is shown in Table 1 that the selectivity factor ($\alpha_{Anth/Phe}$) increases with increasing surface porphyrin loading (e.g., the ''normal'' phases with surface coverage of 1.18 $\mu mol/m^2$ and 2.27 $\mu mol/m^2$ have higher selectivity factor than ''normal'' phase with 0.62 $\mu mol/m^2$ and 0.26 $\mu mol/m^2$ surface coverage). Similarly, $\alpha_{Anth/Phe}$ on ''spread'' phases also are higher on FeProP-silica with greater surface coverage. However, when comparing the ''normal'' phase and the ''spread'' phase with similar surface coverage (e.g., normal-1 and spread-4; normal-2 and spread-2), the $\alpha_{Anth/Phe}$ on all ''spread'' phases were higher, indicating an increase in resolving power when surface porphyrin distribution is more homogeneous. Peak efficiency for phenanthrene and anthracene on different phases with similar surface coverage were also compared and are listed in Table 1. It is clear that column efficiency for these solutes does relate to the homogeneity of porphyrin distribution on silica surface. In general, ''normal'' phases exhibit lower efficiency than ''spread'' phases. This could be because porphyrin aggregation on ''normal'' phases is more severe, and such phases are usually less homogeneous. When one compares the ''spread'' phases with similar porphyrin coverage but different initial amine coverage (e.g., spread-1 and spread-2; spread-3 and spread-4 in Table 1), it appears that the lower amine coverage results in greater band efficiency. This further supports our view that inhomogeneous distribution of porphyrin on silica surface is the reason for peak tailing and band broadening, since the lower the amine coverage, the less porphyrin aggregation is possible.

The difference in synthetic approaches used to prepare the FeProP-silica phases appears to account for the differences observed in the efficiency observed. The ''normal'' FeProP-silica phases were synthesized by first reacting silica gel with 3-aminopropyltriethoxysilane to form aminopropyl-silica. Porphyrin was activated and then reacted with the aminopropyl-silica to yield the ProP-silica. Excess porphyrin (0.1 *M* in reaction mixture) was used to obtain a consistent surface coverage of porphyrin. At such concentration, however, it is known that ProP not only forms dimerization type aggregates in solution, it can also associate to more extensive aggregate structures [14]; hence, clusters of aggregated porphyrins could be immobilized covalently due to the high amine content of the silica (see Table 1 and Fig. 1A). In contrast, for the ''spread'' phase synthesis, the amino groups on surface were distributed evenly by mixing the aminopropyltriethoxysilane with methyltrimethoxysilane. Although the

porphyrins can still aggregate in solution, once immobilized on the surface, the chance for the porphyrin species to remain in close proximity to each other is greatly reduced owing to the lower density of amine sites. Any non-covalently bound aggregated porphyrin species is washed away from the surface by using a π-electron rich solvent (e.g., toluene). This likely results in a phase where the porphyrins are more evenly spaced over the silica surface (see Fig. 1B).

In the case of the ''dilute'' FeProP-silica phase, covalent attachment of ProP was achieved by reacting the normal aminopropyl-silica (amine coverage= 4.36 μmol/m^2) with an extremely dilute activated porphyrin solution (~10^{-3} *M*). Although the amine density on the surface of silica is high, dilution of the porphyrin concentration during the immobilization reaction will decrease the number and size of any aggregates; hence, porphyrins will be randomly immobilized, but with the possibility of two or more porphyrin species still being close enough to interact with each other via a surface aggregate type structure (see Fig. 1C). The net result is that such phases behave somewhere in between the two extremes of ''normal'' and ''spread'' materials.

Although the ''spread'' porphyrin phases exhibit improved column resolution and peak efficiency, the plate numbers obtained on all of the porphyrin-silica phases tested here are still much lower than on most commercial columns. This is likely due to the columns being packed in our laboratory using less than state-of-the-art packing equipment, and to the fact that the desorption ''off'' rate constants for some of the larger PAHs is relatively slow. Such slow desorption kinetics were recently confirmed in this laboratory via bulk phase experiments in which the ProP-silica materials were used as selective preconcentration phases for PAHs [21].

The influence of the specific silica silanization procedure employed on the chromatographic behavior of the Fe(III)ProP-silica stationary phases was also examined. Wirth et al. have found that for monomeric derivatization of the silica particles, by copolymerizing C_{18} and C_1 terminal silanizing agents on the silica surface, a more homogeneous monolayer of C_{18} can be obtained, with surface silanol groups completely blocked [9]. This resulted in a C_{18}-silica phase that exhibited significantly enhanced efficiencies for certain solutes that are subject to hydrogen bonding with surface silanols. These researchers also suggested that using an ethyl instead of a methyl spacer group would not have the same effect because the length of the ethyl chain sterically prevents complete coverage of the underlying silanol groups. Although their goal was primarily to shield the silanol groups on the surface, their silanization procedure is similar to that used in this work to dilute amine sites on the silica surface. Therefore, both methyltrimethoxysilane (C_1) and ethyltrimethoxysilane (C_2) were investigated as reagents for the synthesis of ''spread'' phases. It was found that there was no significant difference in the chromatographic behavior of the porphyrin-silica materials resulting from these two reactions with respect to separation of PAHs (data not shown). Although conditions (water content) were not controlled carefully in the preparation of these materials to ensure monomeric surface derivatization in each case, the enhanced chromatographic behavior of the ''spread'' FeProP-silica phases described above is, nonetheless, more likely due to the specific distribution of the ProP species on the silica surface rather than any effect of shielding silanol groups on the surface. However, further testing of the ''spread'' FeProP-silica phases using other test solutes (peptides and proteins) may be helpful in assessing whether the use of methyltriethoxysilane (vs. ethyltriethoxysilane) as a spreading agent will yield more efficient phases for the separation of such solutes.

3.2. Band profile of perylene on various Fe(III)ProP-silica materials indicate that ''spread'' phases are more homogeneous

The homogeneity of the silica surface can be better understood by studying the phase equilibrium between the two phases (mobile and stationary) and the influence of various parameters, especially the concentration of solute, on this equilibrium. If a stationary phase has only one type of interaction site with the solute, and the concentration of solute is low relative to the total adsorption sites (less than 0.1 m*M*), the equilibrium of the injected solute between the two phases will be a linear function [19], and the retention time for the solute band should not change

as a function of injected concentration. However, if retention times and peak symmetry change appreciably as one increases the injected concentration of solute this would indicate the presence of competitive/multiple interaction site(s).

To assess the homogeneity of ''spread'' and ''normal'' FeProP-silica phases, the chromatographic band profiles of perylene at different injected sample concentrations (0.1 g/l, 0.05 g/l, 0.02 g/l, 0.005 g/l, 0.0001 g/l, 0.00005 g/l) were obtained on different Fe(III)ProP-silica phases. Relatively low solute concentrations were used to avoid fully overloading the column. In order to detect the low concentration solute sample, fluorescence instead of UV detection was used because of its high sensitivity. The chromatograms for perylene on the columns packed with ''spread'' and ''normal'' phases are shown in Fig. 3. As shown, the retention time of perylene changed little on ''spread-4'', while on ''normal-1'' with similar porphyrin coverage, the retention time changed from 2.9 min to 3.2 min when the concentration changed from 0.1 g/l to 0.00005 g/l. On the ''normal-2'' phase with porphyrin coverage of 0.62 μmol/m^2, the retention time changed from 3.2 min to 3.8 min for the same concentration change (the peak of the lowest concentration sample was too broad to be observed visually). Even though ''spread-4'' and ''normal-1'' phases have nearly the same amount of porphyrin on the surface, the band profile of perylene at varying injected concentrations is quite different on the two columns indicating the presence of at least two or more distinctly different interaction sites on the ''normal-1'' phase, while the ''spread-4'' phase appears to possess a more uniform single interaction site. This experiment further supports the notion that the porphyrin distribution on silica surface are significantly different in the ''spread'' and ''normal'' phases.

3.3. Influence of spreading porphyrin sites on shape selectivity

The ''normal'' protoporphyrin-silica phases have been shown previously to exhibit the highest shape selectivity ever reported for planar vs. non-planar PAHs [7]. To assess the shape selectivity of phases synthesized by the new ''spread'' procedure, standard reference material (SRM) 869 was used [20]. SRM 869 is an acetonitrile solution containing three PAH solutes: benzo[*a*]pyrene (BaP), 1,2:3,4:5,6:7,8-

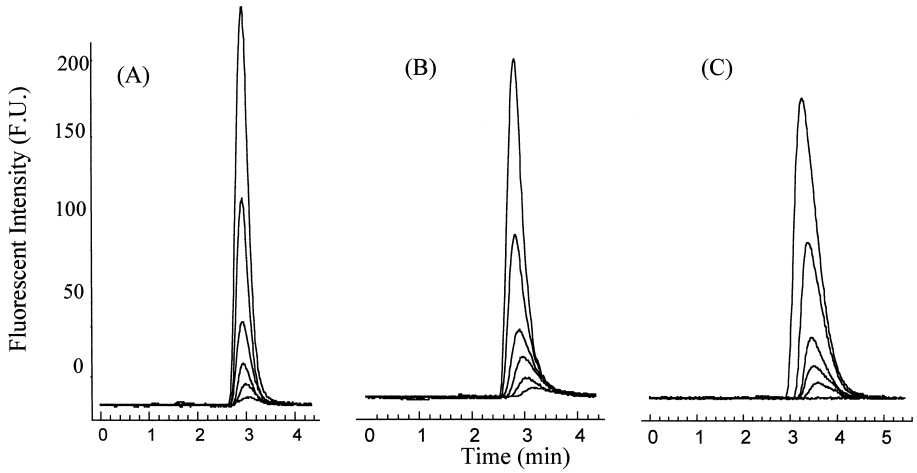

Fig. 3. Band shape as a function of injected perylene concentration on FeProP-silica phases. (A) ''Spread-4'' phases with coverage (cov) of 0.20 μmol/m^2; (B) ''normal-1'' phase (cov=0.26 μmol/m^2); (C) ''normal-2'' phase (cov=0.62 μmol/m^2). Acetonitrile–water content in mobile phase for (A) and (B): 80:20; for (C): 90:10. Sample: perylene in methanol: 0.1 g/l, 0.05 g/l, 0.02 g/l, 0.005 g/l, 0.0001 g/l, 0.00005 g/l. Fluorescence detection: excitation at 290 nm, emission at 430 nm.

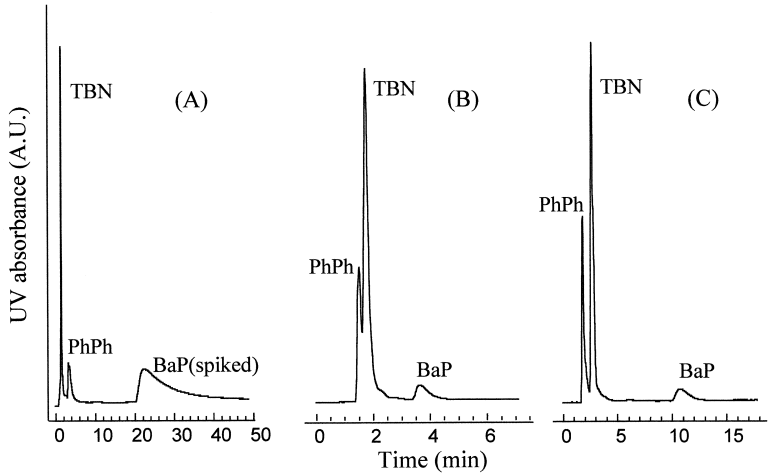

Fig. 4. Separation of SRM 869 on various FeProP-silica phases using 100% acetonitrile as mobile phase. (A) ''Normal-3'' phase with coverage of 1.18 μmol/m^2; (B) ''normal-2'' with coverage of 0.62 μmol/m^2; (C) ''spread-1'' phase with coverage of 0.85 μmol/m^2.

tetrabenzonaphthalene (TBN) and phenanthro[3,4-*c*]phenanthrene (PhPh). The selectivity factor $\alpha_{TBN/BaP}$ (an indicator of shape selectivity of planar vs. non-planar molecule) has been shown to vary with phase type [22], the chemical property of the bonded ligand and phase density, etc. In general, among alkyl-bonded silicas, polymeric C_{18} phases have better shape selectivity with $\alpha_{TBN/BaP}<1.0$, while phases prepared using limited polymeric synthesis or prepared with highly reactive monomeric synthesis routes may result in intermediate shape selectivity, i.e., $1.0<\alpha_{TBN/BaP}<1.7$.

The separation of the SRM 869 was performed on columns packed with the different FeProP-silica phases (Fig. 4 and Table 2). Both the ''spread'' and ''normal'' phases exhibited far better shape selectivity than normal C_{18} phases ($\alpha_{TBN/BaP}$ less than 0.5). Once again columns packed with the ''spread'' ProP-silica materials exhibited improved PAH separation. Better peak efficiency and less peak tailing were observed with the ''spread'' phase (Fig. 4). In addition to yielding better chromatographic performance, ''spread'' phases also retain a high degree of shape selectivity for planar PAHs, (e.g., with $\alpha_{BaP/PhPh}=15.7$ on a ''spread'' phase (coverage of 0.85 μmol/m^2) compared to 1.5–2.7 on a polymeric

Table 2
Comparison of shape selectivity on various stationary phases using SRM 869

	Selectivity factors		
	$\alpha_{(BaP/PhPh)}$	$\alpha_{(BaP/TBN)}$	$\alpha_{(TBN/PhPh)}$
Normal FeProP-silica (1.18)[a]	39.3	8.7	2.5×10^{-2}
Normal FeProP-silica (0.62)[a]	6.9	4.2	0.24
Spread FeProP-silica (0.85)[a]	15.7	6.7	0.17
Monomeric C_{18}[b]	0.8	0.5	0.6
Polymeric C_{18}[b]	1.5–2.7	0.5–2.0	0.6–0.7
Ion pairing acridine[c]	4.2	2.2	1.85

[a] Mobile phase: 100% acetonitrile, data measured in our laboratory.
[b] Mobile phase: acetonitrile–water (85:15) [20].
[c] Mobile phase: 100% acetonitrile [23].

C_{18} phase [20]). The selectivity values reported here are also greater than the values reported recently for the same PAH pairs by Chu et al. on an acridine phase formed by ion pairing interaction between acridine and the stationary support [23].

3.4. Coupled redox/UV–Vis absorbance method as a qualitative indicator of porphyrin distribution on the surface

Development of a method to fully characterize any chemically modified silica stationary phase material is a challenging task. To date, physical methods such as Raman spectroscopy, electron spin resonance, electronic spectroscopy and solid-state NMR have been used successfully to characterize silica materials derivatized with alkyl groups and other species [24–27]. However, the strong UV–Vis absorbance of porphyrins makes questions about their distribution on the surface potentially addressable by examining differences in the UV–Vis spectra of such immobilized species. While a diffuse reflectance measurement would be the preferred approach to obtain the spectra of the porphyrins on silica, it has been found that merely taking the spectrum of a FeProP-silica slurry can be used to gain qualitative information about the distribution of porphyrins on the silica surface.

The significant difference in the visible bands for iron(III)- and iron(II)-protoporphyrin has been utilized recently to monitor the redox state of iron within immobilized protoporphyrins on silica [17]. The typical α- and β-bands formed upon reduction of ferriporphyrins (as utilized for the determination of hemes as pyridine hemochromes [16]) are known to sharpen in detergent as compared to aqueous alkali, probably due to a change to monomers promoted by the interaction of the detergent with the metalloporphyrin. The same behavior is observed for ferroporphyrin immobilized on silica gel (obtained in situ by adding sodium hydrosulfite crystals to a slurry of ferriporphyrin silica in water or lauryl sulfate–NaOH, and obtaining a spectrum of a suspension of the particles). The α- and β-bands of Fe(II)ProP-silica showed two distinctive peaks at 547 nm and 558 nm, respectively. Because of the concern for stability of Fe(II)ProP-silica in air, the spectrum of this material was taken immediately after the Fe(III) center of Fe(III)ProP-silica was reduced to Fe(II) in situ by sodium hydrosulfite. In Fig. 5, the spectra of various ferriporphyrin-silicas together with the respective chromatograms of PAH separations on these phases are compared. Phases prepared by the ''spread'' method [''spread-1'', cov=0.85 $\mu mol/m^2$ in Table 1 (Fig. 5(I)-A)] were found to display much more distinguished α- and β-bands than the ''normal'' packing material [''normal-2'', cov=0.62 $\mu mol/m^2$ and ''normal-3'', cov=1.18 $\mu mol/m^2$ in Table 1 (Fig. 5(I)-B and (I)-C)]. More interestingly, the chromatogram for PAH separation on the ''spread-1'' phase also showed better resolution and efficiency than the ''normal-2'' and ''normal-3'' [Fig. 5(II)-A, (II)-B and (II)-C], indicating a correlation between the band shapes of the UV–Vis spectrum and the chromatographic behavior of the stationary phase.

This result suggests a more homogeneous distribution of the porphyrins on the surface of the ''spread'' phase compared to the ''normal'' phase. Indeed, it is known that aggregation of porphyrins via π–π interactions or by bridging ligands can cause significant change in the UV–Vis spectrum in solution [14]. It is reasonable, therefore, that covalently bonded porphyrin species would behave similarly. As shown, the extinction coefficient of the α- and β-bands appear to be directly related to the distribution of porphyrin on surface. Pasternack et al. [28] have characterized the spectral changes of porphyrins in terms of a monomer-dimer model. For protoporphyrin, the monomer and the dimer have Soret bands (~400 nm) at approximately the same wavelength, but with different molar absorptivities. Gallagher and Elliott [29] have studied aggregation in 0.02 *M* NaOH and found that the Soret band was much more sensitive to changes from dimer to monomer than was the Q-band region. Still, only when the concentration was over 100 μ*M*, can a shift in λ_{max} of the Soret band be observed. However, change of λ_{max} in the Q bands was not obvious even at higher concentrations (over 1000 μ*M*). Only the changes in extinction coefficient were observed for changes in this range. In most of the studies associated with protoporphyrin, it was found that the extinction coefficient changes when the porphyrin changes from a dimer to monomer, with monomers having a higher extinction coefficient in general.

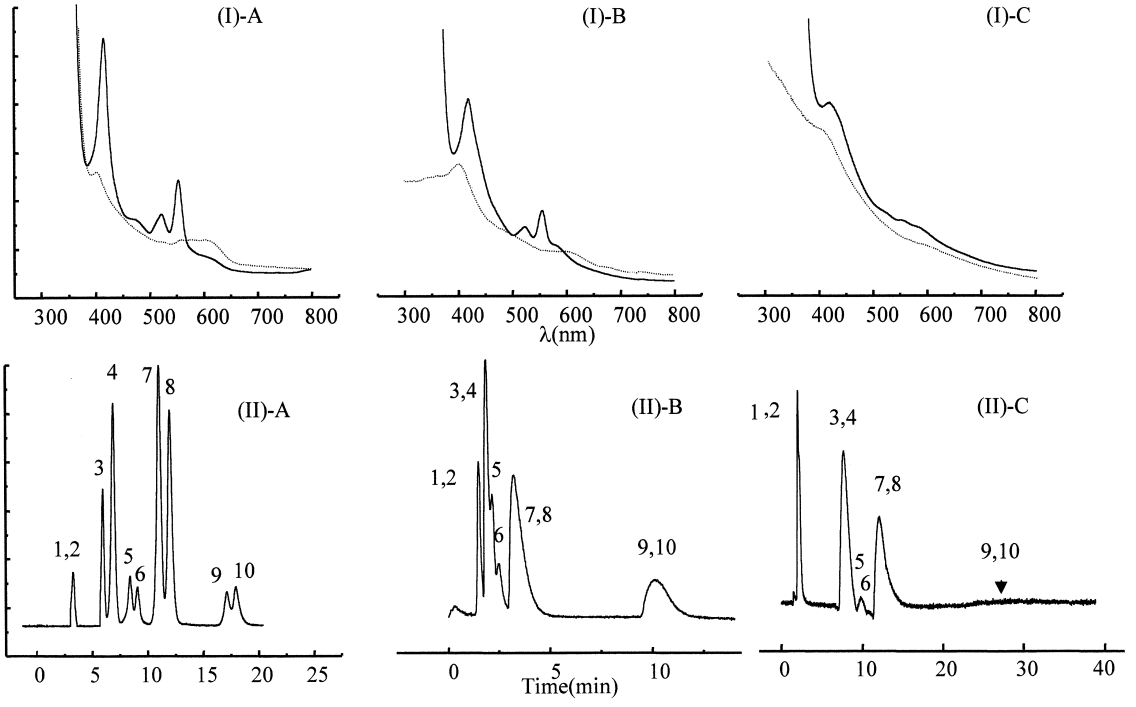

Fig. 5. (I) UV absorbance spectra of various Fe(II)ProP-silicas (—) and Fe(III)ProP-silicas (···); (I)-A: ''spread-1'' phase with coverage of 0.85 μmol/m^2; (I)-B: ''normal-2'' phase with coverage of 0.62 μmol/m^2; (I)-C: ''normal-3'' phase with coverage of 1.18 μmol/m^2. (II) PAH separation on respective FeProP-silica phases for which UV–Vis spectra are reported in (I) above: (II)-A: ''spread-1'' phase with coverage of 0.85 μmol/m^2; (II)-B: ''normal-2'' phase with coverage of 0.62 μmol/m^2; (II)-C: ''normal-3'' phase with coverage of 1.18 μmol/m^2. Sample composition: (1) naphthalene, (2) biphenyl, (3) 1,1-binaphthyl, (4) anthracene, (5) pyrene, (6) benz[*a*]anthracene, (7) triphenylene, (8) chrysene, (9) perylene, (10) benzo[*a*]pyrene. Mobile phase: acetonitrile–water (50:50) step to 100% acetonitrile in 10 min. UV detection at 254 nm, flow-rate: 1 ml/min.

These previous results for solution phase porphyrin aggregation help to explain the lack of λ_{max} shifts observed for the Q bands here in case of FeProP-silica. Indeed, the same behavior is also observed for porphyrins on silica surfaces. With the higher possibility of aggregation on ''normal'' phases, the porphyrins were very likely to aggregate on the surface in a form of dimers or more extensive aggregates. Thus the ''extinction coefficient'' is lowered in those cases, resulting in less distinguishable α- and β-bands in the UV spectrum of ferriporphyrin-silica. In contrast, on the ''spread'' phase, the degree of aggregation or dimer formation was limited, thus a higher extinction coefficient and more easily distinguished α- and β-bands are observed. In any case, the change in Soret band followed the trend in the α- and β-bands: the extinction coefficient increases when aggregation decreases. By examining a number of FeProP-silica phases with different surface coverages and aggregation, a semi-quantitative result was obtained to correlate the peak/valley ratio of the band at 580 nm with the porphyrin distribution on silica surface (data not shown). Indeed, this coupled redox/spectroscopy method can be used to examine the porphyrin distribution on silica surface prior to packing a column, therefore enabling a prediction regarding the ultimate chromatographic performances of a given stationary phase.

4. Conclusions

In summary, it has been shown that the chromatographic efficiencies of novel protoporphyrin-silica phases with respect to PAH separations can be improved measurably by altering the method of

porphyrin immobilization. This is accomplished by more evenly spacing the porphyrin species on the surface of the silica via dilution of pendant amine sites used to covalently link the ProP species to the solid support. The results suggest that the alternative method of ProP immobilization yields a more homogeneous stationary phase with respect to the thermodynamics and possibly kinetics of solute interaction. This finding with ProP-silica, coupled with recent results indicating that the selectivity and efficiency of related tetraphenylporphyrin-silicas for fullerene separation can be dramatically enhanced by using a different immobilization chemistry [30], strongly suggests that further improvements in the performance of columns packed with porphyrin-silica materials are possible with additional modifications in the linking chemistry. Given the unique solute selectivities already demonstrated on such materials, such improvements in chromatographic performance should make the use of these columns more attractive for given applications.

Acknowledgements

The authors acknowledge Dr. Lane Sander from the National Institute of Standard Technology for the generous gift of SRM 869. The authors also wish to thank Erich Steinle for proofreading this manuscript.

References

[1] R. Brindle, K.J. Albert, Chromatographia 757 (1997) 3.
[2] K. Jinno, T. Nagoshi, N. Tanaka, M. Okamoto, J.C. Fetzer, W.R. Biggs, J. Chromatogr. 392 (1987) 75.
[3] K. Jinno, K. Yamamoto, T. Ueda, H. Nagashima, K. Itoh, J. Chromatogr. 594 (1992) 105.
[4] Y. Saito, K. Jinno, J.J. Pesek, Chromatographia 38 (1994) 295.
[5] J.J. Kirkland, J.L. Glajch, R.D. Farlee, Anal. Chem. 61 (1989) 2.
[6] J. Xiao, M. Meyerhoff, Anal. Chem. 68 (1996) 2818.
[7] S. Chen, M. Meyerhoff, Anal. Chem. 70 (1998) 2523.
[8] J. Xiao, C.E. Kibbey, D.E. Coutant, G.B. Martin, M.E. Meyerhoff, J. Liq. Chromatogr. Rel. Technol. 19 (1996) 2766.
[9] M.J. Wirth, R.W.P. Fairbank, H.O. Fatunmbi, Science 275 (1997) 44.
[10] L.C. Sander, S.A. Wise, Anal. Chem. 67 (1995) 3284.
[11] M.J. Wirth, H.O. Fatunmbi, Anal. Chem. 65 (1993) 822.
[12] T. Fornstedt, G. Zhong, G. Guiochon, J. Chromatogr. A 742 (1996) 55.
[13] T. Fornstedt, G. Zhong, G. Guiochon, J. Chromatogr. A 741 (1996) 12.
[14] W.I. White, in: D. Dolphin (Ed.), The Porphyrins, Physical Chemistry, Part C, Vol. 5, Academic Press, New York, 1978, p. 303.
[15] C.E. Kibbey, M.E. Meyerhoff, Anal. Chem. 65 (1993) 2189.
[16] J.E. Falk, Porphyrins and Metalloporphyrins: Their General, Physical, and Coordination Chemistry, and Laboratory Methods, Elsevier, Amsterdam, 1964.
[17] U. Ruedel, M.E. Meyerhoff, Anal. Chim. Acta 392 (1999) 191.
[18] L.C. Sander, R.M. Parris, S.A. Wise, Anal. Chem. 63 (1991) 2589.
[19] G. Guiochon, S.G. Shirazi (Eds.), Fundamentals of Preparative and Nonlinear Chromatography, Academic Press, New York, 1990, p. 55.
[20] Certificate of Standard Reference Material 869, National Institute of Standards and Technology, Gaithersburgh, MD, 28 March 1990.
[21] S. Chen, M. Meyerhoff, presented at the 50th Pittsburgh Conference, Orlando, FL, 5–12 March 1999, paper 2291P.
[22] L.C. Sander, S.A. Wise, Anal. Chem. 59 (1987) 2309.
[23] J. Chu, T. Takeuchi, T. Miwa, Anal. Chim. Acta 370 (1998) 125.
[24] M. Ho, M. Cai, J.E. Pemberton, Anal. Chem. 69 (1997) 2613.
[25] C. Miller, R. Dadoo, R.G. Kooser, J. Gorse, J. Chromatogr. 458 (1988) 255.
[26] S.C. Rutan, J.M. Harris, J. Chromatogr. A 656 (1993) 197.
[27] K.B. Sentell, J. Chromatogr. A 656 (1993) 231.
[28] R.F. Pasternack, P.R. Huber, P. Boyd, G. Engaser, L. Francesconi, E. Gibbs, P. Fasella, G.C. Venturo, L. de C. Hinds, J. Am. Chem. Soc. 94 (1972) 4511.
[29] W.A. Gallagher, W.B. Elliott, Ann. NY Acad. Sci. 206 (1973) 463.
[30] D.E. Coutant, S.A. Clark, A.H. Francis, M.E. Meyerhoff, J. Chromatogr. 824 (1998) 147.